Polarimetric radar discrimination between small, large, and giant hail at S band.

(Picca, J., and A. Ryzhkov)

I. Discrimination between small and large hail. Previous version of the algorithm.

The previous version of the algorithm for hail detection and determination of its size which was delivered to the Lincoln lab in September 2010 aimed at discrimination between small (less than 2.5 cm) and large (more than 2.5 cm) hail using a set of thresholds involving radar reflectivity factor Z and differential reflectivity Z_{DR}. Depending on the height of the radar resolution volume, different Z and Z_{DR} thresholds have to be applied. A functional description of the previous algorithm is included herein.

1. Run the existing HCA and identify the areas recognized as "rain / hail mixture"
2. Identify large hail in the areas of rain / hail mixture using the following rules.

(1) Determine the height of freezing level (H_{FL}) either as a height of the melting layer top from the WSR-88D MLDA or from the RUC model.
(2) Determine the height of the center of the radar resolution volume H using range and elevation.
(3) Use different rules for recognizing large hail for different values of the difference $H - H_{FL}$:

Large hail is recognized if

$Z > 60$ dBZ if $H > H_{FL}$

$Z > 60$ dBZ and $Z_{DR} < 0.5$ dB if $0 < H_{FL} - H < 1$ km

$Z > 62$ dBZ and $Z_{DR} < 1.5$ dB if $1 < H_{FL} - H < 2$ km (1)

$Z > 59$ dBZ and $Z_{DR} < 1.9$ dB if $2 < H_{FL} - H < 3$ km

$Z > 57$ dBZ and $Z_{DR} < 2.3$ dB if $H_{FL} - H > 3$ km

II. Validation of the hail size discrimination rules. Considerations for developing an advanced version of the algorithm for discrimination between hailstones of different sizes.

a) *Ground validation*

The rules (1) which constitute original version of the algorithm for determination of hail size were based primarily on the results of theoretical modeling of the hail melting process. During last year, analysis of polarimetric signatures in hailstorms producing hail of different size has been performed using the data collected by the KOUN WSR-88D radar in central Oklahoma. Six hail-bearing storms (March 27, 2009, May 10, 2010, May

16, 2010, May 20, 2010, April 14, 2011, and May 24, 2011) were examined. These storms produced hail ranging in size from 1.9 cm to 11 cm. The most extreme hail case occurred on May 16, 2010 inflicting significant damage in the downtown of Oklahoma City. It became the subject of a separate study by Picca and Ryzhkov (2010, 2011). Abundant ground truth is available for this hailstorm. In other cases, ground truth was much scarcer, although it was possible to draw certain conclusions about the difference between vertical profiles of key polarimetric variables Z, Z_{DR}, and ρ_{hv} associated with hail of various sizes (Kaltenboeck and Ryzhkov 2011). Notably, in both studies polarimetric signatures of hailstorms simultaneously observed by the S-band KOUN WSR-88D and C-band OU-PRIME radars are compared.

Very large hail with sizes exceeding 5 cm has been observed in 4 examined cases and it was found that the "giant hail" (with D > 5 cm) can be distinguished from hail of smaller sizes capitalizing on a pronounced depression of the cross-correlation coefficient ρ_{hv} in the hail-generation zone above the freezing level and the combined information provided by Z, Z_{DR}, and ρ_{hv} below the freezing level (e.g., Kumjian et al. 2010, this year 1st quarter report to the Lincoln Lab). Therefore, in a more advanced version of the hail size determination algorithm described in this annual report, a new category of giant hail is added to the categories of small and large hail.

The essence of validation results is illustrated in Figs. 1 – 4. Six scatterplots ($Z\text{-}Z_{DR}$, Z_{DR} - H_{DR} , $Z\text{-}\rho_{hv}$, $Z_{DR}\text{-}\rho_{hv}$, $Z\text{-}K_{DP}$, and $Z_{DR}\text{-}K_{DP}$) showing radar data from the 0.5˚ scans at locations of hail reports during the extreme hailstorm in Oklahoma City on May 16, 2010 are presented in Fig. 1. Different symbols in the scatterplots indicate three categories of corresponding hail size from surface reports. For every hail report, the radar data with Z > 55 dBZ within a spatial / temporal domain of 1km x 1° x 6 min centered on the report location have been selected. This creates 200+ data points for only 13 reports. Furthermore, as report time errors on the order of a few minutes could negatively impact the analysis, the 13 reports were segregated into three size categories (D < 3 cm, 3 cm ≤ D < 5 cm, D ≥ 5 cm), instead of using specific hail sizes. At 0.5° antenna elevation, the height of the center of the radar resolution volume at locations corresponding to ground hail reports was within the range 2 – 3 km below the freezing level.

In the $Z\text{-}Z_{DR}$ and $Z\text{-}\rho_{hv}$ plots (Fig. 1a,c), there is a clear trend of larger hail sizes towards increasing Z and decreasing Z_{DR} or ρ_{hv}. Fig. 1a reveals that when Z > 65 dBZ and Z_{DR} < 1 dB, all data points correspond to giant hail reports. However, where Z is 55 – 65 dBZ and Z_{DR} is 0 – 2 dB, there is a wide array of hail sizes reported on the ground pointing to the need of using a fuzzy logic approach rather than a set of rigid rules / thresholds for appropriate classification of hail of different sizes. Notably, high Z_{DR} exceeding 2 dB are found for hail sizes of 2.5 and 4.4 cm within the range of Z between 55 and 63 dBZ, which shows that even 4.4 cm hail can be overwhelmed by the presence of smaller, melting hailstones and very large raindrops with high intrinsic Z_{DR}.

The $Z\text{-}\rho_{hv}$ scatterplot shows the benefit of using ρ_{hv} in combination with Z (Fig. 1c). When Z > 65 dBZ and ρ_{hv} < 0.95, all data points correspond to giant hail reports. Yet again, there is a wide distribution of hail sizes if Z is between 55and 65 dBZ and ρ_{hv} is between 0.90 and 0.96. Finally, the $Z_{DR}\text{-}\rho_{hv}$ scatterplot suggests the utilization of both Z_{DR} and ρ_{hv} along with Z to estimate hail size most accurately (Fig. 1d). A clear trend of larger hail sizes associated with lower Z_{DR} and ρ_{hv} values exists. None of small (less than

2.5 cm) hail reports are associated with Z_{DR} and ρ_{hv} values less than 1 dB and 0.95, respectively. On the other hand, a majority of the "giant hail" reports match Z_{DR} less than 1 dB and ρ_{hv} less than 0.96.

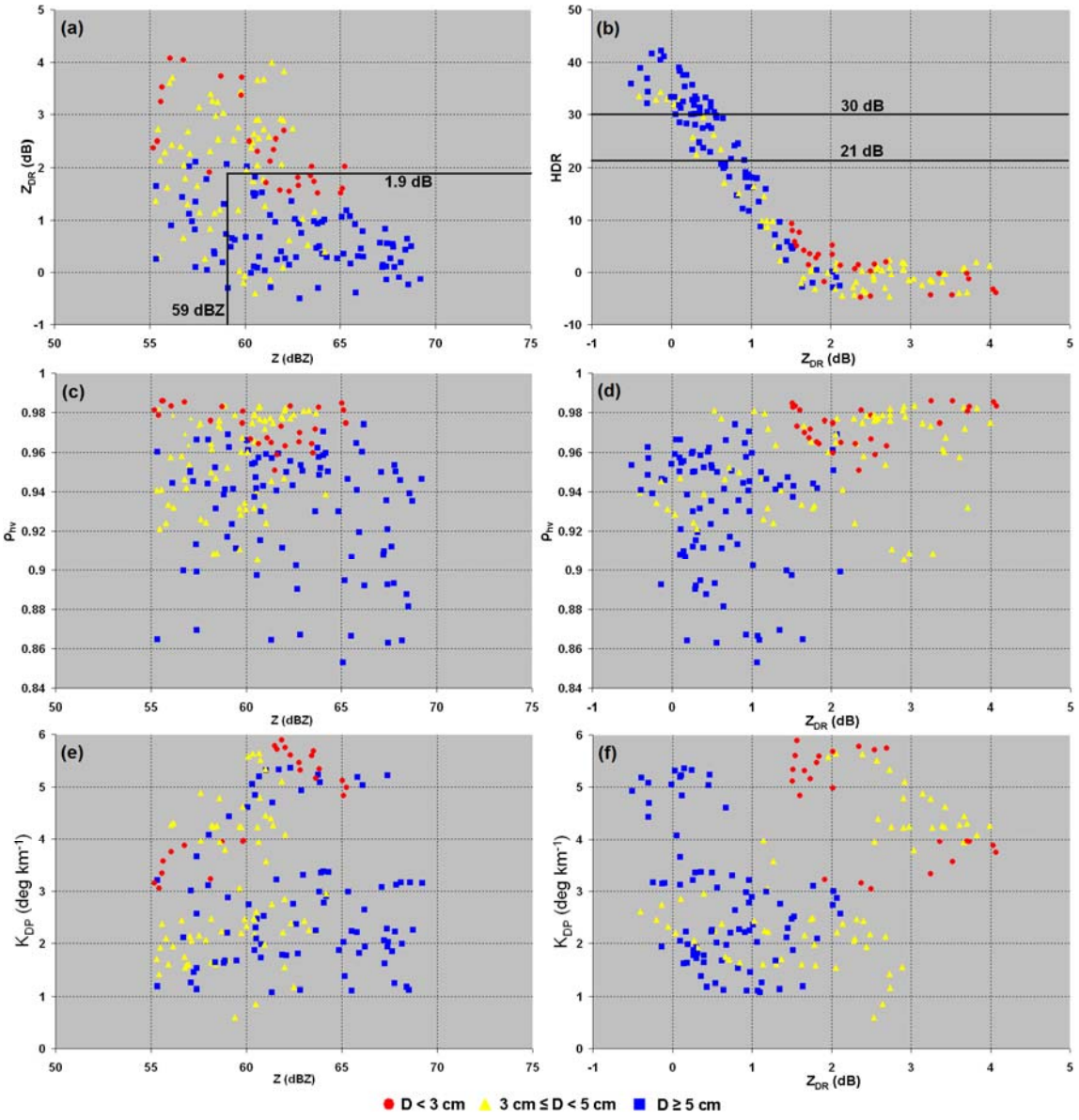

Fig. 1. Scatterplots of (a) Z vs Z_{DR}, (b) Z_{DR} vs H_{DR}, (c) Z vs ρ_{hv}, (d) Z_{DR} vs ρ_{hv}, (e) Z vs K_{DP}, and (f) Z_{DR} vs K_{DP} measured at S band for 13 reports, segregated into three size categories (D < 3 cm; 3 cm ≤ D < 5 cm; D ≥ 5 cm), between 2058 and 2129 UTC across the Oklahoma City metro area. Solid black lines in (a) indicate threshold for large hail detection for beam heights between 2 and 3 km below the freezing level according to Ryzhkov et al. (2010), while in (b) they indicate the thresholds for 1.9 cm hail (21 dB line; NWS old large hail definition) and damaging hail (30 dB line) detection according to Depue et al. (2007)

Fig. 2 illustrates significant reduction of the cross-correlation coefficient above the freezing level if giant hail grows in the wet growth regime. The area of depressed ρ_{hv} descends once giant hail starts falling out of the hail generation zone. The signature is more pronounced at C band.

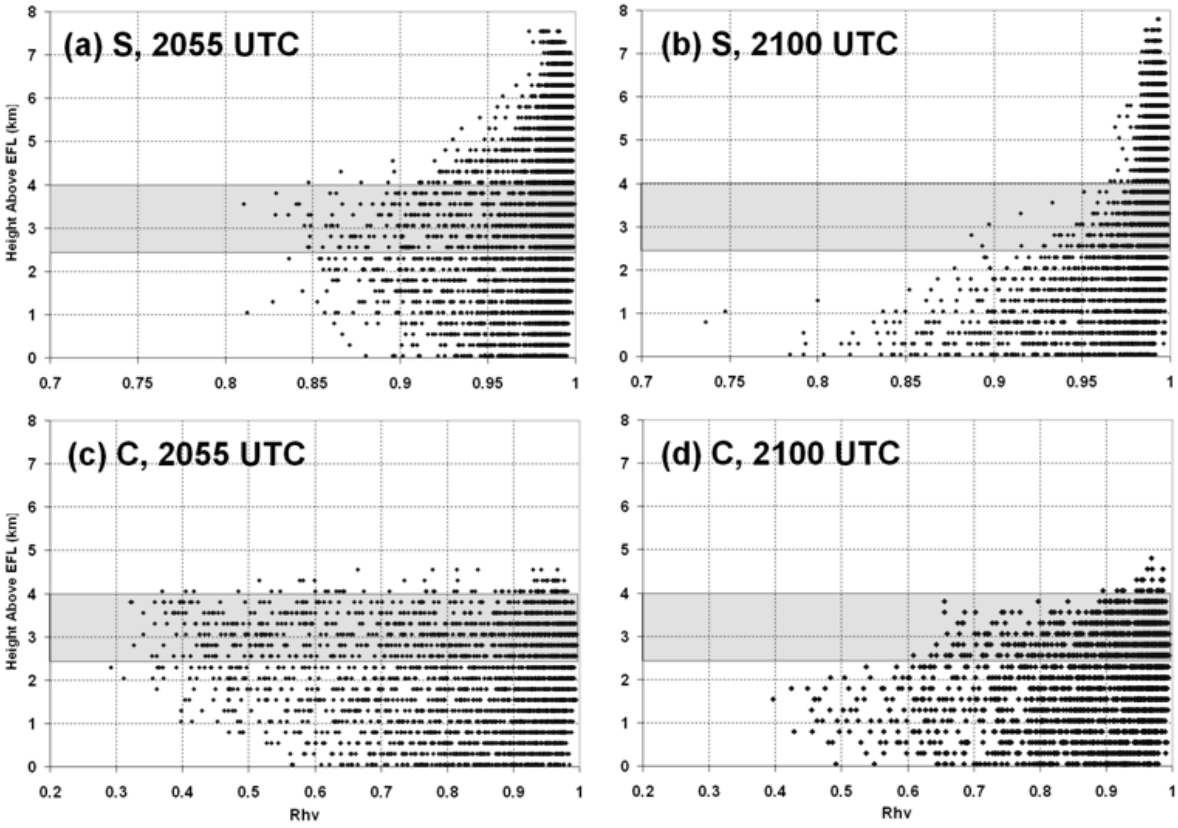

Fig. 2. Cross-correlation coefficient values above the environmental freezing level (EFL) within the 50-dBZ contour for KOUN at (a) 2055 UTC and (b) 2100 UTC, and OU-PRIME at (c) 2055 UTC and (d) 2100 UTC. The highlighted region represents the approximate layer of -10˚C to -20˚C using a surface-based parcel from the 17 May 2010 Norman, OK sounding at 0000 UTC.

Average vertical profiles of Z, Z_{DR}, and ρ_{hv} at S and C bands within the regions of Z exceeding 55 dBZ for the storms with maximal hail sizes 2 cm and 10 cm reported on the ground are displayed in Fig. 3. It is interesting that the differences in Z_{DR} and ρ_{hv} for the hail of small and giant sizes are much more pronounced than the corresponding differences in Z. The plots in Fig. 3 were used to specify parameters of the membership functions in different height intervals in the proposed version of the algorithm for determination of hail size.

b) *Considerations for developing an advanced version of the algorithm for discrimination between hail of different sizes*

The results of theoretical and observational analysis of the past year dictate the need for a more advanced and sophisticated version of the hail classification algorithm which is built on the principles of fuzzy logic rather than rigid threshold / rules and is

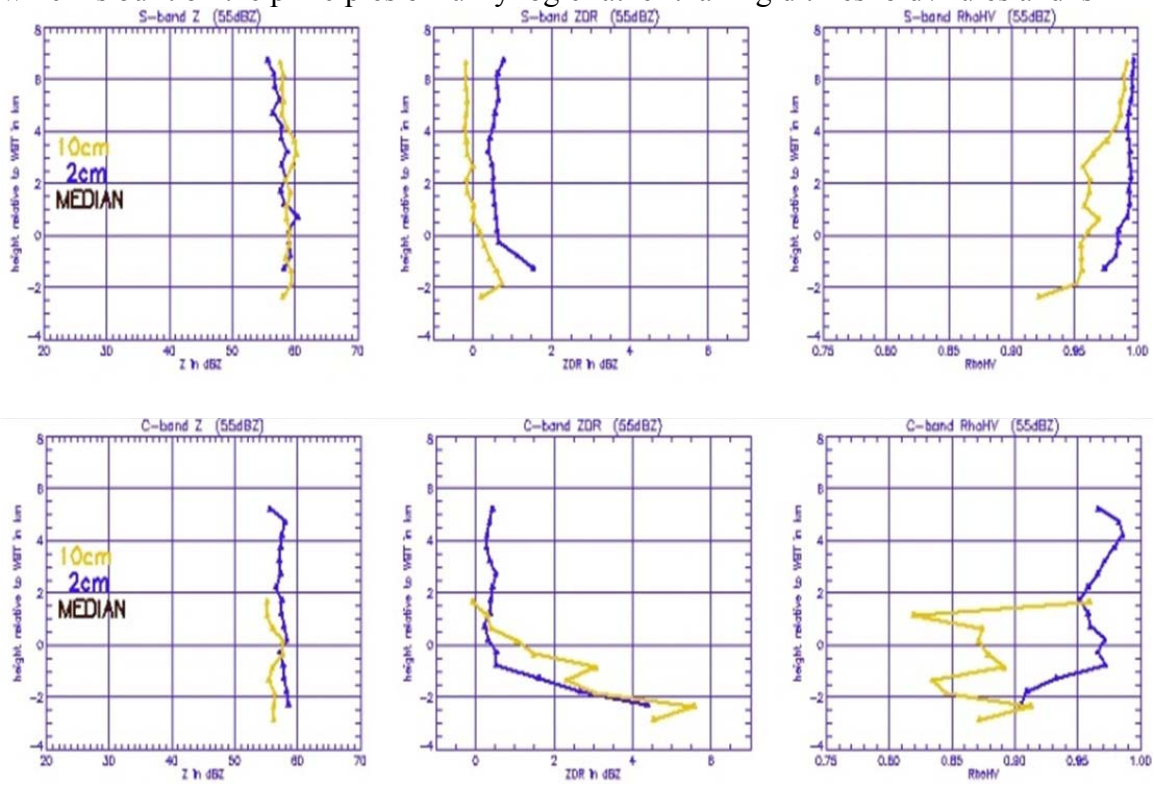

Fig. 3. Average vertical profiles of Z, Z_{DR}, and ρ_{hv} within regions of Z > 55 dBZ for cases with 2 cm and 10 cm hail size observed simultaneously by S-band and C-band polarimetric radars. The heights are shown with respect to the level of zero wet bulb temperature where melting of hail starts.

designed for distinguishing between three categories of hail size: small (D < 2.5 cm), large (2.5 cm < D < 5 cm), and giant (D > 5 cm). The idea is to split the class category "hail mixed with rain" (RH) in the current WSR-88D HCA into three classes of hail. A separate fuzzy logic routine for discrimination between three classes of hail should be applied in the areas designated as RH by the existing WSR-88D HCA described in Park et al. (2009). Here is a summary of important features of the proposed classification algorithm.

(1) The algorithm will utilize three polarimetric variables: Z, Z_{DR}, and ρ_{hv} instead of two (Z and Z_{DR}) in the previous version of the algorithm.
(2) The membership functions have trapezoidal shape determined by 4 parameters x_1 – x_4 as in Park et al. (2009).
(3) The parameters of the membership functions are different for each of the 6 height intervals depending on the altitudes of the 0°C and -25°C level of the wet bulb temperature. Height intervals are specified in the titles of Tables 1 – 6 where the parameters of the membership functions are listed (section III).

(4) Parameters x3 of the membership functions for Z and Z_{DR} are consistent with original hard thresholds in the previous algorithm described in section I.
(5) It is taken into account that for a given maximal hail size Z has maximum slightly below the freezing level in the steady state model of melting hail (Ryzhkov et al. 2009). Z_{DR} can be slightly negative for giant hail above the freezing level. Below the freezing level where wet bulb temperature T_w is equal to 0°C, Z_{DR} increases almost linearly with decreasing height within first 2 km below the freezing level and then increases with slower pace beneath. In each height interval below the freezing level, Z increases and Z_{DR} and ρ_{hv} decrease as hail size increases.
(6) At altitudes above the T_w = -25°C level, the discrimination between different hail sizes is made solely on Z, so the membership functions for Z_{DR} and ρ_{hv} are the same for all three hail size categories.
(7) The width of the membership functions was determined taking into account the observed variability of radar parameters for a given size category of hail shown in Fig. 4.
(8) The confidence vector Q in Eq (2) is the same as in the main HCA algorithm and is determined in the main HCA module.
(9) For simplicity, the elements of the matrix W in Eq (2) are set to unity.
(10) Many entries in the tables are "first guess" estimates which require further refining / tuning as part of future validation efforts.

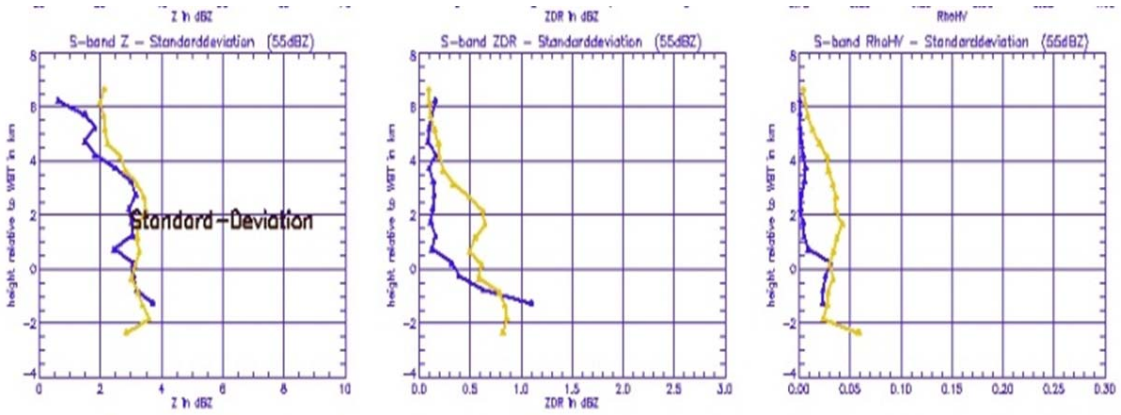

Fig. 4. Vertical profiles of standard deviations in the estimates of average Z, Z_{DR}, and ρ_{hv} within the 55 dBZ region at S band for two hail cases illustrated in Fig. 3.

III. Functional description of the algorithm for discrimination between small, large, and giant hail

1. Run the existing WSR-88D HCA described in Park et al. (2009) and identify the regions recognized as "rain/hail mixture (RH)".
2. For any given gate / pixel classified as RH, determine the height of the corresponding center of the radar resolution volume and find out to which of the six height intervals it belongs. The intervals are defined in the titles of tables 1 – 6.

3. A fuzzy logic routine for discrimination between 3 classes (small, large, and giant hail) contingent on the height interval is applied. As in the case of the standard WSR-88D HCA, the procedure implies computation of aggregation values for each of the three classes as

$$A_i = \frac{\sum_{j=1}^{3} W_{ij} Q_j P^{(i)}(V_j)}{\sum_{j=1}^{3} W_{ij} Q_j} \quad i = 1,2,3 \qquad (2)$$

where $P^{(i)}(V_j)$ is a membership function (which characterizes the distribution of the j^{th} variable for the i^{th} class), W_{ij} is a weight between 0 and 1assigned to the i^{th} class and the j^{th} variable, and Q_j is an element of the confidence vector assigned to the j^{th} variables. The classification decision is based on the maximal aggregation value. In our classification scheme, $V_1 = Z$, $V_2 = Z_{DR}$, $V_3 = \rho_{hv}$, the elements of the confidence vector **Q** are determined in the main HCA, and the elements of the matrix **W** are set to 1 for a time being. The membership functions for hail in 3 size categories are determined similarly to Park et al. (2009), i.e., as trapezoids defined by parameters $x_1 – x_4$ specified in Tables 1 – 6 for each height interval. The membership functions are displayed in Figs. 5 – 7.

Table 1. $H > H(T_w = -25°)$. T_w is wet bulb temperature.

	Small hail	Large hail	Giant hail
P(Z(dBZ))			
x_1	45	55	55
x_2	50	60	65
x_3	60	65	75
x_4	65	70	80
$P(Z_{DR}(dB))$			
x_1	-0.5	-0.5	-0.5
x_2	-0.3	-0.3	-0.3
x_3	0.3	0.3	0.3
x_4	0.5	0.5	0.5
$P(\rho_{hv})$			
x_1	0.92	0.92	0.92
x_2	0.96	0.96	0.96
x_3	0.99	0.99	0.99
x_4	1.0	1.0	1.0

Table 2. $H(T_w = 0°) < H < H(T_w = -25°)$

	Small hail	Large hail	Giant hail
P(Z(dBZ))			
X1	45	55	55

X2	50	60	65
X3	60	65	75
X4	65	70	80
$P(Z_{DR}(dB))$			
X1	-0.5	-0.5	-0.7
X2	-0.3	-0.3	-0.4
X3	0.3	0.3	0.2
X4	0.5	0.5	0.5
$P(\rho_{hv})$			
X1	0.92	0.85	0.80
X2	0.96	0.90	0.85
X3	0.99	0.96	0.93
X4	1.0	0.98	0.98

Table 3. $H(T_w = 0°) - 1\ km < H < H(T_w = 0°)$

	Small hail	Large hail	Giant hail
P(Z(dBZ))			
X1	45	55	55
X2	50	60	65
X3	60	65	75
X4	65	70	80
$P(Z_{DR}(dB))$			
X1	-0.1	-0.3	-0.6
X2	0.3	0.1	-0.2
X3	0.7	0.5	0.2
X4	1.2	1.0	0.7
$P(\rho_{hv})$			
X1	0.93	0.86	0.80
X2	0.96	0.91	0.86
X3	0.99	0.97	0.94
X4	1.0	0.98	0.98

Table 4. $H(T_w = 0°) - 2\ km < H < H(T_w = 0°) - 1\ km$

	Small hail	Large hail	Giant hail
P(Z(dBZ))			
X1	45	52	57
X2	52	62	67
X3	62	67	77
X4	67	72	80
$P(Z_{DR}(dB))$			
X1	0.5	0.3	-0.3

X2	0.9	0.6	0.1
X3	1.6	1.5	0.8
X4	2.6	2.3	1.3
$P(\rho_{hv})$			
X1	0.94	0.87	0.80
X2	0.96	0.91	0.87
X3	0.98	0.97	0.95
X4	1.0	0.98	0.98

Table 5. $H(T_w = 0°) - 3$ km $< H < H(T_w = 0°) - 2$ km

	Small hail	Large hail	Giant hail
P(Z(dBZ))			
X1	45	54	54
X2	49	59	64
X3	59	64	74
X4	64	69	80
$P(Z_{DR}(dB))$			
X1	1.0	0.4	0.0
X2	1.5	0.9	0.5
X3	2.5	1.9	1.5
X4	4.0	3.5	2.0
$P(\rho_{hv})$			
X1	0.94	0.88	0.80
X2	0.96	0.92	0.88
X3	0.98	0.98	0.96
X4	0.99	0.99	0.98

Table 6. $H < H(T_w = 0°) - 3$ km

	Small hail	Large hail	Giant hail
P(Z(dBZ))			
X1	45	52	52
X2	47	57	62
X3	57	62	72
X4	62	67	80
$P(Z_{DR}(dB))$			
X1	1.2	0.6	0.2
X2	1.6	1.1	0.7
X3	2.7	2.3	1.7
X4	4.5	4.0	2.2
$P(\rho_{hv})$			

X1	0.94	0.88	0.80
X2	0.96	0.92	0.88
X3	0.98	0.98	0.96
X4	0.99	0.99	0.98

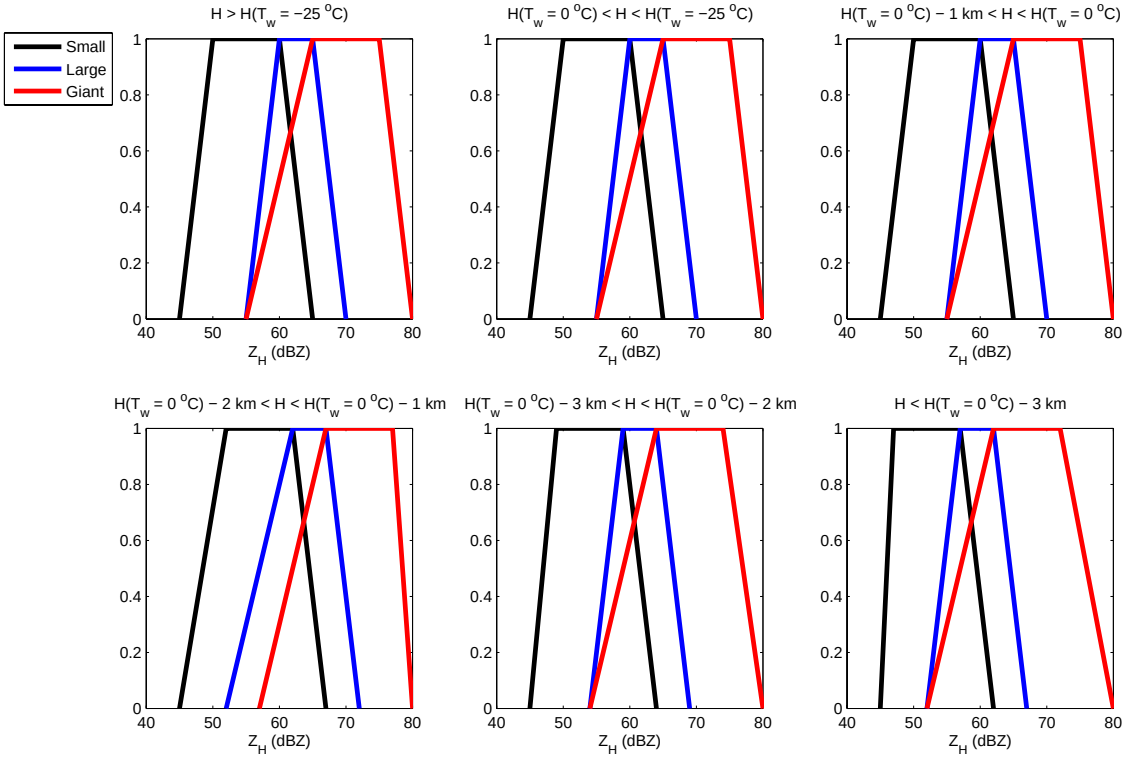

Fig. 5. Trapezoidal membership functions for Z_H. Black = small hail, Blue = large hail, red = giant hail.

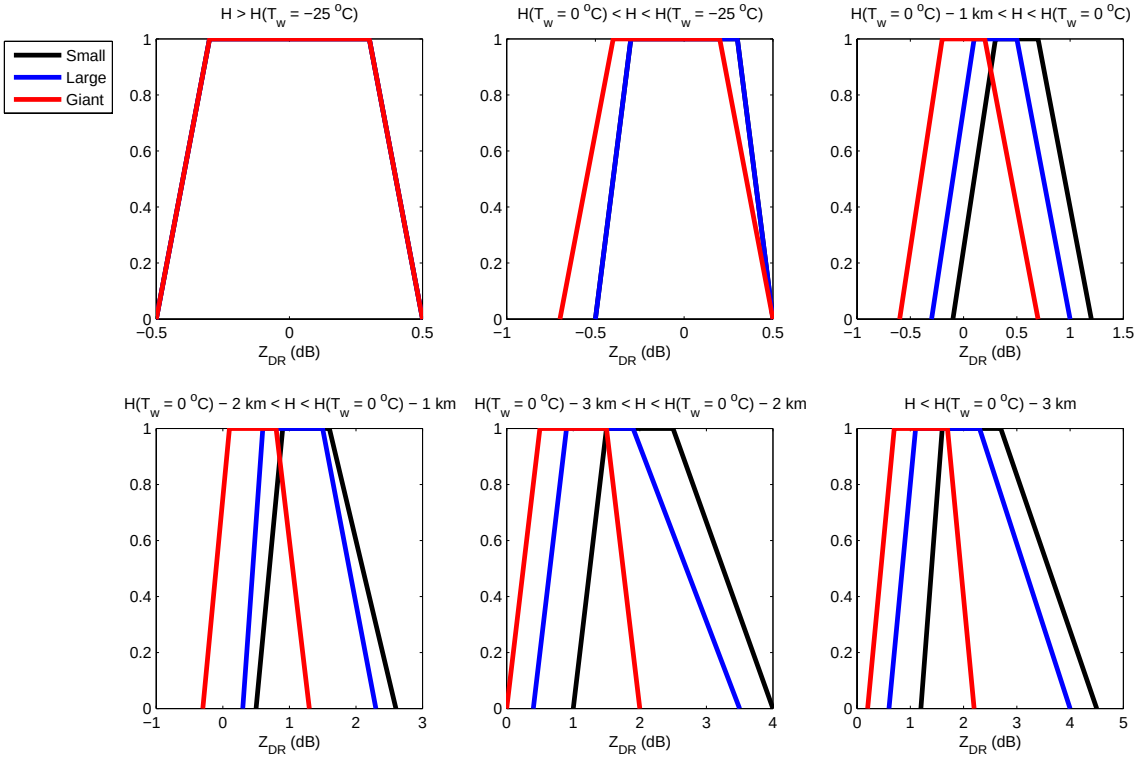

Fig. 6. Trapezoidal membership functions for Z_{DR}. Black = small hail, Blue = large hail, red = giant hail.

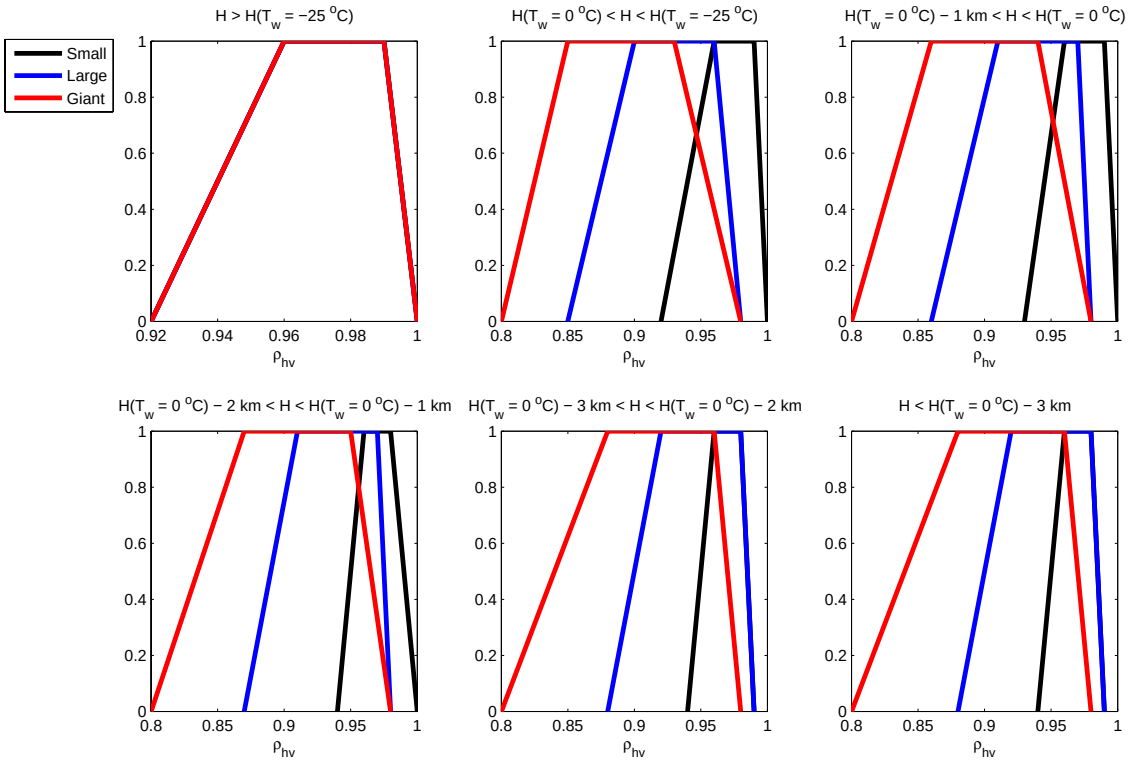

Fig. 7. Trapezoidal membership functions for ρ_{hv}. Black = small hail, Blue = large hail, red = giant hail.

References

1. Depue, T.K., P.C. Kennedy, and S.A. Rutledge, 2007: Performance of the hail differential reflectivity (H_{DR}) polarimetric radar hail indicator. *J. Appl. Meteor. Climat.*, **46**, 1290-1301.
2. Kaltenboeck, R., and A. Ryzhkov, 2011: Severe hail size discrimination using dual-polarized weather radar data. A dual-wavelength comparison between C and S band. 6th European Conference on Severe Storms, October, Spain, 4pp.
3. Kumjian, M., J. Picca, S. Ganson, A. Ryzhkov, J. Krause, D. Zrnic, and A. Khain, 2010: Polarimetric characteristics of large hail. *25th Conference on Severe Local Storms.* Denver, CO, Amer. Meteor. Soc., 11.2.
4. Park, H-S., A. V. Ryzhkov, D. S. Zrnic, and K. E. Kim, 2009: The hydrometeor classification for the polarimetric WSR-88D; description and application to an MCS. *Wea. Forecasting*, **24,** 730-748.
5. Picca, J., and A. Ryzhkov, 2010: A multiple-wavelength polarimetric analysis of the 16 May 2010 Oklahoma City extreme hailstorm. *25th Conference on Severe Local Storms.* Denver, CO, Amer. Meteor. Soc., P8.6.
6. Picca, J., and A. Ryzhkov, 2011: A dual-wavelength polarimetric analysis of the May 16, 2010 Oklahoma City extreme hailstorm. Conditionally accepted by *Monthly Weather Review*.

7. Ryzhkov, A.V., S.M. Ganson, A. Khain, M. Pinksy, and A. Pokrovsky, 2009: Polarimetric characteristics of melting hail at S and C bands. *34th Conf. on Radar Meteorology*, Williamsburg, VA, Amer. Meteor. Soc., 4A.6. Available online at [http://ams.confex.com/ams/34Radar/techprogram/paper_155571.htm].
8. Ryzhkov, A.V., D.S. Zrnic, J. Krause, M.R. Kumjian, and S.M. Ganson, 2010: Discrimination between large and small hail, final report. NOAA/NSSL report, 18 pp. Available online at [http://publications.nssl.noaa.gov/wsr88d_reports/FINAL_HailSize.doc]